THE JOURNAL OF PHYSICAL CHEMISTRY A

pubs.acs.org/JPCA Article

Dissociation of Valine Cluster Cations

Lukas Tiefenthaler, Milan Ončák, Siegfried Kollotzek, Jaroslav Kočišek,* and Paul Scheier*

Cite This: J. Phys. Chem. A 2020, 124, 8439−8445 Read Online

ACCESS | Metrics & More | Article Recommendations | Supporting Information

ABSTRACT: Independently of the preparation method, for cluster cations of aliphatic amino acids, the protonated form M_nH^+ is always the dominant species. This is a surprising fact considering that in the gas phase, they dissociate primarily by the loss of 45 Da, i.e., the loss of the carboxylic group. In the present study, we explore the dissociation dynamics of small valine cluster cations M_n^+ and their protonated counterparts M_nH^+ via collision-induced dissociation experiments and ab initio calculations with the aim to elucidate the formation of M_nH^+-type cations from amino acid clusters. For the first time, we report the preparation of valine cluster cations M_n^+ in laboratory conditions, using a technique of cluster ion assembly inside He droplets. We show that the M_n^+ cations cooled down to He droplet temperature can dissociate to form both $M_{n-1}H^+$ and $[M_n-COOH]^+$ ions. With increasing internal energy, the $M_{n-1}H^+$ formation channel becomes dominant. $M_{n-1}H^+$ ions then fragment nearly exclusively by monomer loss, describing the high abundance of protonated clusters in the mass spectra of amino acid clusters.

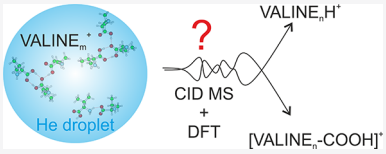

INTRODUCTION

Understanding of physical, chemical, and biological processes in living organisms often requires exploration of fundamental properties of isolated biomolecular ions or their van der Waals complexes. Such exploration is not easy for nonvolatile biomolecules. Standard sublimation approaches result in molecular decomposition or neutral vapor pressures insufficient for ion formation by conventional ionization methods. A significant improvement was brought by invention of the electrospray technique[1] where ions are formed on the liquid/aerosol interface at atmospheric pressure and reach sufficient ion intensities for transport to vacuum and further analysis.[2] However, the control of the ion state in electrospray sources is not trivial and introduces a high level of uncertainty when interpreting the results. Parameters such as solution ions, capillary temperature, collisional activation, and charge transfer processes may result in the formation of excited, isomerized, or metastable ion species far from their electronic or vibrational ground state. Complicated ion transport and trapping systems have to be used to cool the ions for spectroscopy or comparison with theory.[3,4]

In the present study, we are using our recently developed method[5] of ion assembly in He droplets to prepare rather exotic valine dimer cations. In the present technique, all steps of the ion formation are known and well controllable. This makes the technique an ideal ion preparation tool for spectroscopy as well as for studies in combination with theory.

As will be shown in the present study, the He matrix enables stabilization of metastable reaction intermediates. He droplets therefore provide a gas phase alternative to matrix isolation and desorption studies performed on surfaces. The use of He droplets for spectroscopy of reaction intermediates was recently applied, e.g., by Davies et al.[6] or Franke et al.[7] In such studies, the reaction intermediates can be kept inside the He matrix, as He is transparent for incoming light. In our case, the He matrix is removed, enabling application of further techniques of physical chemistry, such as the collision-induced dissociation (CID). Also, in our case, all reaction or dissociation products can be detected. That is not the case of conventional surface desorption techniques, where the species need to overcome a desorption barrier to be detected, and consequently, predominantly low mass decomposition products are usually detected.[8,9]

For the present study, we selected L-valine. Valine is a well-explored aliphatic amino acid with good thermal stability and reasonable vapor pressures for gas phase studies upon sublimation. A number of previous studies have been done with this molecule using various ionization methods in the gas phase,[10,11] clusters,[12] or He droplets,[13−15] describing the chemistry of its cation as well as protonated clusters in detail. Of particular importance is the fact that valine, despite its high stability as a neutral molecule, rapidly releases the carboxylic group upon ionization, i.e., the cation is very unstable. Such behavior is typical for all aliphatic amino acids.[10,16] After clustering with another amino acid, however, the mass spectrum is always dominated by protonated amino acid cluster ions.[12] This occurs also in the case when cluster ions are formed in He droplets.[13−15] Does it mean that the proton transfer reaction is exothermic and the valine cluster cation is only a transient species? We succeeded in stabilization of the stoichiometric cluster cations M_n^+ in He droplets, and we use

Received: August 6, 2020
Revised: September 14, 2020
Published: September 15, 2020

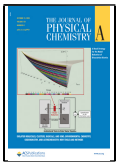

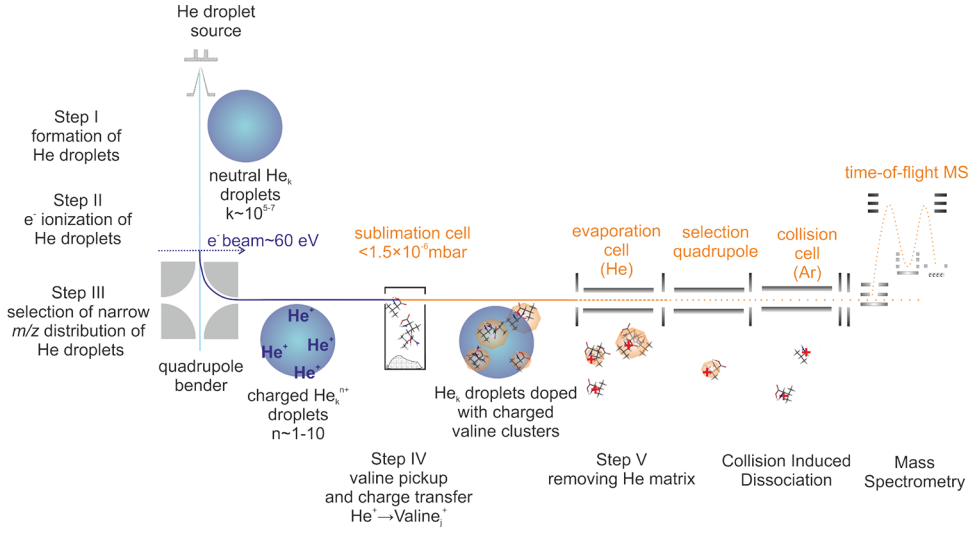

Figure 1. Scheme of the experiment and multistep process of ion assembly in He droplets enabling preparation of cold clusters.

computational modeling to rationalize the MH^+ ion formation from the small clusters as well as stabilization of alphacarbon bonds in its protonated form.

METHODS

Valine cluster cations were prepared by ion assembly in He droplets. The method was recently developed in our laboratory and is described elsewhere.[5] The clusters are analyzed using a modified tandem mass spectrometer (Waters Q-TOF Ultima). For better description of the method, we include Figure 1, which shows the individual cluster ion assembly steps.

In the first step, a continuous He droplet beam source[17] is used at a He stagnation pressure of 20 bar and a nozzle temperature of 9.3 K to produce neutral He droplets with an average size of about 10^6 He atoms.[18] In the second step, the droplets are multiply charged by electron ionization at a controlled electron energy. For the present positive ion mode, we used the electron energy of 60 eV. In the third step, droplets are deflected perpendicularly to the neutral droplet beam by an electrostatic quadrupole ion bender. In the fourth step, amino acid vapor is picked up by charged He droplets, and the charge is transferred from He^+ (IE = 24.59 eV)[19] and resp. He_2^+ (IE = 22.22 eV) cations to valine (IE = 8.9 eV).[11] In the present experiment, we sublimed L-valine (Sigma-Aldrich 99.8%) at temperatures below 110 °C, resulting in a distribution of only small valine cluster ions that we wanted to form. Except for the pickup pressure, as the main parameter, the cluster distribution can be further influenced by the size and charge state of the droplets selected by the quadrupole bender. We also point out that sublimation temperatures needed to observe clustering are much lower than temperatures required in experiments working with coexpansions in molecular beams or conventional neutral He droplet pickup. In comparison to neutral beams, the method is superior because the collision partner required for clustering is the He droplet with a huge collision cross section. In addition, third-body collision is not required to stabilize the initial dimer, as the helium droplet efficiently absorbs its excess energy. In comparison to experiments with neutral He droplets, the method is more efficient because in the present case, droplets are multiply charged, and therefore, several charged clusters can be formed in each droplet.[20] This way, we are able to reach high signals even at very low pickup pressures, which enables studies of cold biomolecular cluster ions. After pickup and charge transfer from He, the cluster ions inside He droplets are cooled down to a few Kelvin.[14,21]

Finally, in the fifth step, the amino acid cluster ions are released from the He matrix by colliding the droplets in an RF-guiding hexapole with room temperature He gas. This step was crucial for the present study. Settings of low evaporation gas pressures allow us to form very cold molecular cluster ions such as complexes of valine with He. Higher evaporation cell pressures allow for complete evaporation of helium or even slight energy transfer to the dopant cluster ions that results in conditions similar to other cluster ion experiments with amino acids. At these conditions, we start to observe the protonated valine clusters. The cases are described in detail in the Results section.

The released cluster ions were analyzed by means of TOF analysis or CID. Details may be found in our recent paper.[22] For CID, we used Ar collision gas at a pressure of $\sim 1 \times 10^{-5}$ mbar in the 9 cm-long RF hexapole collision cell. It is important to mention that despite the low collision cell pressure, CID results presented here are only qualitative. Concerning the relative intensities, it is well known that the transport of the precursor ion through the guiding RF multipoles is much easier than for ions formed by the collisions with Ar atoms with different energies and formation positions. Therefore, the intensities of the fragment ions with respect to the precursor ion are typically underestimated.[23] Additionally, our orthogonal extraction setup has low sensitivity for low mass fragments, and we cannot detect potentially formed H^+ ions. The total ion signal in the CID measurements drops above 5 eV collision energy, which may be caused by the aforementioned fact as well as by the deflection of low mass fragment ions in collisions with the Ar gas. Therefore, the CID curves for individual fragments presented in this work may actually rise steeper and dominate the spectrum at lower energies.

Concerning the energy, temperature effects of the collision gas and more important RF guiding voltages might induce uncertainties in the observed energy up to several eVs.[24,25] Therefore, we can gain again only a qualitative picture, which can be, however, well supported by theory, as discussed below.

https://dx.doi.org/10.1021/acs.jpca.0c07208
J. Phys. Chem. A 2020, 124, 8439−8445

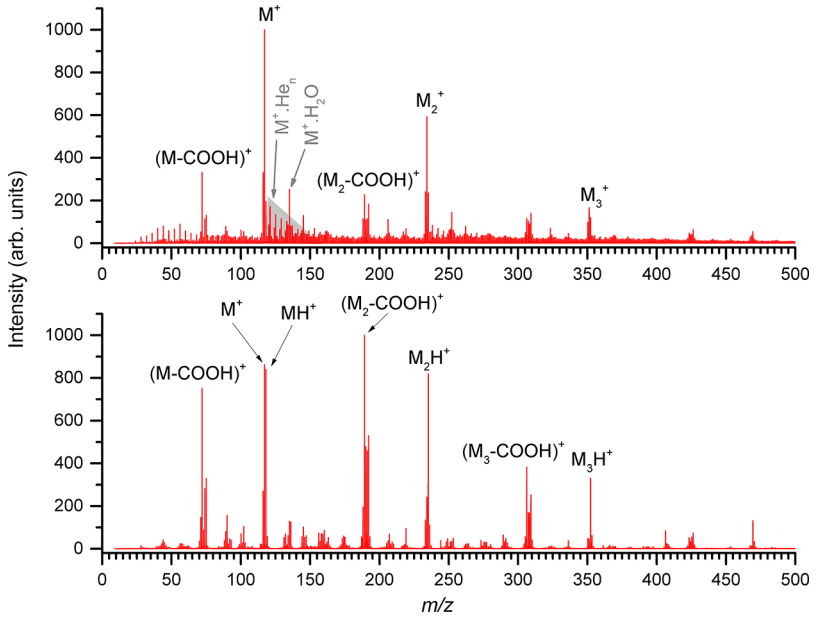

Figure 2. Mass spectra at different evaporation cell conditions and without Ar gas in the collision cell of a Q-TOF instrument. (upper panel) Spectrum at low evaporation cell pressure showing valine and valine cluster ions with attached He from the droplets or water impurities. (bottom panel) All He atoms stripped from the cluster ions and the same fragment ions are observedas reported in previous studies with amino acid doped He droplets.

Experimental results are supported by quantum chemical calculations. Local minima structures and reaction energies of the ions and clusters were described using standard density functional theory (DFT), combining two functionals to obtain an estimate of the calculation error, B3LYP and M06-2X.[26] For B3LYP, the D2 dispersion correction as suggested by Grimme was used,[27] further denoted as B3LYP+D2. Structures with various interaction patterns were optimized. All structures represent local minima, and zero-point correction is included in all reported energies. Calculations were performed utilizing the Gaussian quantum chemical software.[28]

RESULTS AND DISCUSSION

In the present study, we focus on small valine cluster cations. Clusters were prepared inside He droplets and liberated from the host droplets via collisions with He gas in the evaporation cell of the instrument. The intensity of the liberation process can be controlled by the pressure inside the evaporation cell. Two typical cases are shown in Figure 2.

The top panel of the figure shows a mass spectrum at a low pressure inside the evaporation cell. Under these conditions, the collisional activation only evaporates He from the droplet, and cold dopant cluster ions are extracted from the He matrix in their original form. Our understanding of the cluster formation process is that the first picked up valine molecule is ionized by charge transfer from He^+ and the formed cation is quenched by the He matrix. Further, valine molecules assemble to a cluster around this ionic core. The He droplet provides a heat sink during the whole cluster ion formation process. For some of the ions, which were extracted to the time-of-flight mass spectrometer, we can even see that a few He atoms remain attached to the ion. At the same time, however, we can already observe some fragmentation via neutral loss of 45 Da. We will discuss the details of the process below.

In the bottom panel of Figure 2, we can see the case when higher He pressure inside the evaporation cell was used. Here, the He matrix is completely removed, and the dopant cluster ions gain further energy in collisions with He atoms in the RF ion guide. We can see that even though there is still some amount of monomers M^+, the clusters are predominantly in their protonated form M_nH^+. Neutral loss of 45 Da now dominates the mass spectrum.

To explore the dissociation of valine clusters, we used collision-induced dissociation with argon gas. The relative intensities of the main fragment ions observed after CID of valine dimer and trimer cations as a function of collision energy in the lab frame (upper axis) and the center of the mass frame (bottom axis) are plotted in Figures 3 and 4, respectively. Note that the CID results are only qualitative, as discussed in the Methods section.

From the upper panel of Figure 3, we can see that ions corresponding to neutral loss of 45 Da from the valine dimer Val_2^+ cation are formed already at low collision energies; a threshold for their formation cannot be detected in the present experiment. The precursor parent cations may even be in a transient state, metastable with respect to dissociation via this channel. This channel competes with the MH^+ channel, which strongly increases and dominates the spectrum at collision energies between 2.5 and 5 eV. At energies above 6 eV, m/z = 72 fragments dominate the spectrum. In the case of the trimer in Figure 4, we can see a similar fragmentation pattern, and additional fragments are only due to further monomer evaporation occuring at higher collision energies.

For the protonated valine dimer Val_2H^+ at low energies, the only significant fragmentation channel is monomer loss, which results in the formation of MH^+. At higher collision energies, the spectrum is dominated by m/z = 72 cations, $[M-COOH]^+$, as in the previous case. However, the fragmentation toward the $[M-COOH]^+$ cation has an energy threshold around 1 eV higher than in the case of Val_2^+. The same fragmentation channels are observed also for the protonated trimer in Figure 4, plus channels corresponding to additional monomer loss. The channel corresponding to the neutral loss

https://dx.doi.org/10.1021/acs.jpca.0c07208
J. Phys. Chem. A 2020, 124, 8439−8445

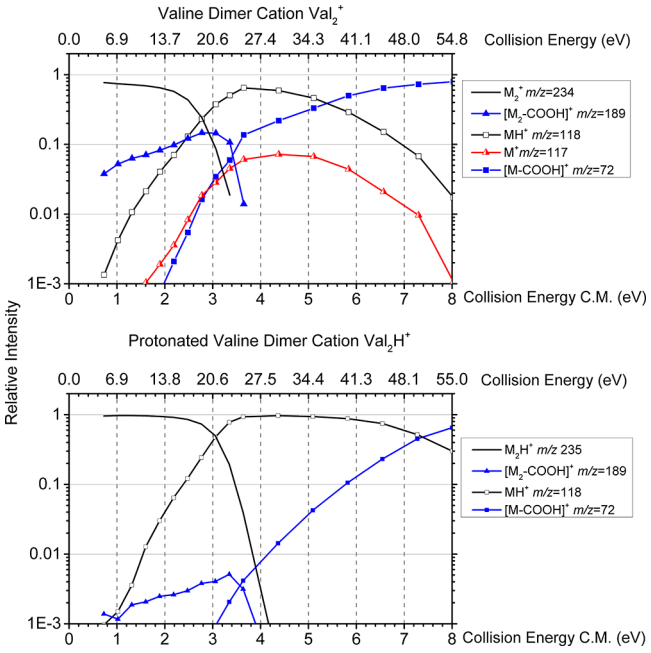

Figure 3. Relative intensities of individual product ions after CID of valine dimer cations and protonated valine dimers as a function of collision energy in the center of the mass frame.

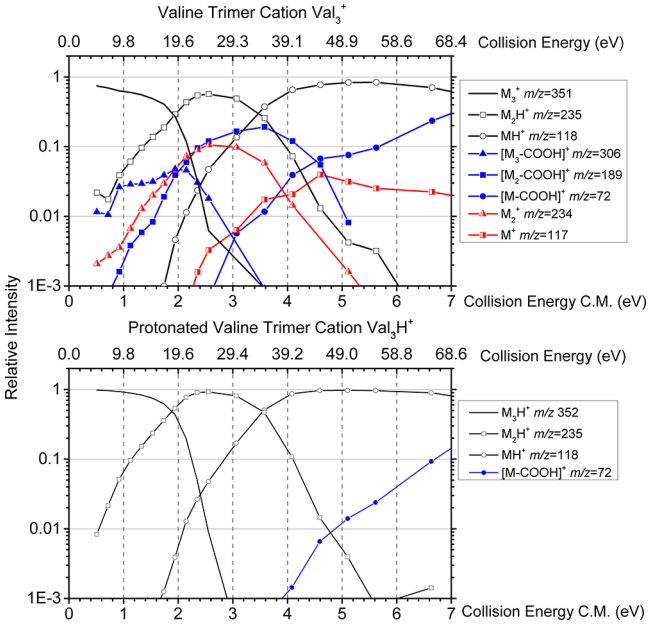

Figure 4. Relative intensities of individual product ions after CID of valine trimer cations and protonated valine trimers as a function of the collision energy in the center of the mass frame.

of 46 Da, HCOOH loss, is detected with only negligible intensity.

Let us compare the observed behavior with theoretical reaction energies for the formation of individual fragment ions. In both M_2^+ and M_2H^+, the charge is almost completely localized on one unit (about 90% within the CHELPG analysis[29]). We can see in Figure 5a that dissociation of valine dimer cations to form protonated monomers is energetically favored compared to the simple monomer loss leading to M^+ cations, with a difference of nearly 1 eV. At the same time, we can see in Figure 5b that the protonated dimer M_2H^+ is very stable, and while MH^+ can be formed from it at around 1.4 eV, the channel leading to M^+ requires an energy input of more than 4 eV. The situation is the same for the trimer, shown in Figure 5c,d, with all energies lowered so that the $M_2H^+ + [M-H]$ channel becomes exothermic. This shift of the reaction energy is in a good agreement with the CID spectrum presented in Figure 4. To demonstrate that the shift is not caused only by a different reduced mass in the case of the trimer, we include also the laboratory frame collision energies in Figures 3 and 4. These findings explain well the M_nH^+ cation production after ionization of amino acid clusters. While $M_{s-1}H^+$ formation from M_s^+ needs only a very small energetic input or it is exothermic for larger clusters, $M_{s-1}H^+$ ions are stable against dissociation, with a possible product $M_{s-2}H^+$ but with the M_{s-2}^+ channel practically closed. It is worth to mention that the lowest reaction energy for the formation of $M_{s-1}H^+$ ions from M_s^+ is achieved for the case that the neutral coproduct has a dissociated form of $CO_2 + C_4NH_{10}$.

Concerning the loss of the carboxylic group, Figure 5 shows that the channel requires slightly more energy than the channel leading to $M_{n-1}H^+$, but the dissociation of HCOOH is favored compared to the monomer loss for protonated valine clusters M_nH^+. These thermodynamic data may rationalize the $[M_n-COOH]^+$ ion signal in the observed mass spectrum (Figure 2) without collision gas (low internal energy) as a sequential process. M_n^+ efficiently dissociates to MH^+, which may have enough energy to further dissociate by HCOOH loss. However, at higher excitation energies, as studied using CID in Figures 3 and 4, the internal energy of the clusters will be enough to open the monomer evaporation channel.

In the case of larger clusters, the differences in reaction energies are even more pronounced. For trimer M_3^+, the M_2H^+ formation channel is exothermic and 0.6 eV below the $[M_3-COOH]^+$ channel. For the protonated trimer, the monomer loss (M_2H^+ formation channel) lies 0.1 eV above the $[M_3-COOH]^+$ channel. The $[M_n-COOH]^+$ fragments may therefore form by dissociation of M_{n+1}^+ precursor ions. This is well supported by the CID spectrum for the trimer in the top panel of Figure 4, where the $[M_2-COOH]^+$ ions form from low collision energies below 1 eV and become the second most intense fragmentation channel at around 2 eV.

This sequential process, however, cannot explain the CID spectrum of M_2^+ at low collision energies shown in Figure 3. The neutral loss of 45 Da dominates the ion yield at low energies, which is in a good agreement with the observed mass spectrum shown in Figure 2. The experimental data therefore suggests that the threshold energy for the COOH loss is lower than that of [M−H] loss or that at low energies, the COOH loss channel may be preferred due to dynamical reasons. Both COOH loss and [M−H] loss channels can be reached by direct dissociation from the most stable M_2^+ isomer as shown in Figure 5. The relative rate of both channels will depend on entropic factors as well as M_2^+ isomer distribution in the experimental mixture. Some of the M_2^+ clusters selected for CID analysis can even have the form of a He matrix-stabilized $[M-H]\cdot MH^+$ or $M[M-COOH]^+\cdot COOH$ complexes. In the initial cluster formation step inside He droplets, a picked up valine molecule is ionized by charge transfer from He_2^+. The resulting cation may be in an excited electronic state or undergo dissociation after which the dissociation products form a complex stabilized by He. Such matrix-stabilized complexes are not included in our analysis shown in Figure 5. Dissociation of HCOOH from isolated protonated amino acids

https://dx.doi.org/10.1021/acs.jpca.0c07208
J. Phys. Chem. A 2020, 124, 8439−8445

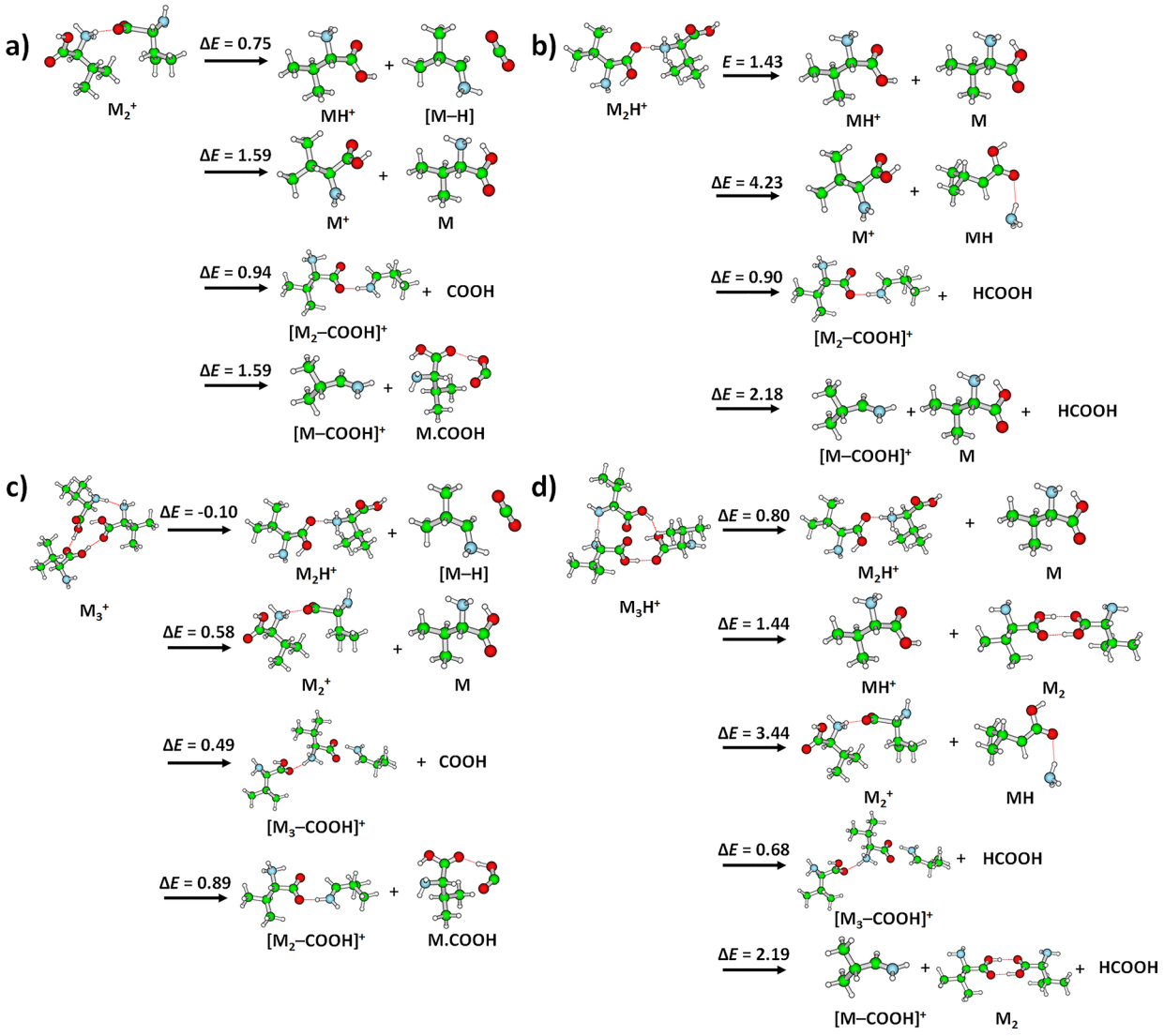

Figure 5. (a–d) Dissociation reactions of valine dimers and protonated valine dimer cations. Calculated at the B3LYP+D2/aug-cc-pVDZ level of theory. M06-2X/aug-cc-pVDZ results are included for comparison in the Supporting Information. Color code: carbon - green, oxygen - red, nitrogen - blue, and hydrogen - white.

was, e.g., rationalized by neutral water loss.[30,31] Unambiguous identification of the structure of the Val_2^+ complexes stabilized inside He droplets may be, however, provided only by further experimental studies using spectroscopic techniques. The fact that a part of the valine cluster cations could be stabilized in the form of its reaction intermediates demonstrates that He droplets may be well used as an alternative to the matrix isolation studies on surfaces.

CONCLUSIONS

We performed an experimental study of small valine cluster cations allowing a comparison with theory. Using cluster ion assembly in He droplets, we succeed to stabilize the stochiometric M_n^+ cations before fragmentation to the usually observed M_nH^+ cluster ion series. M_n^+ dissociates primarily via the loss of CO_2 and C_4NH_{10} resulting in the formation of $M_{(n-1)}H^+$. Protonated M_nH^+ dissociates nearly exclusively by evaporation of monomer units. Only at higher energies, depending on the cluster size, formation of the $[M-COOH]^+$ cation (m/z = 72) may occur. This is describing well the formation of protonated amino acid clusters using various ionization techniques.

Aliphatic amino acids exhibit a particularly intense COOH loss fragmentation channel. Our data indicate that $[M_n-COOH]^+$ ions are mainly formed in a sequential process from M_{n+1}^+ precursor clusters. Reaction energies for direct dissociation of a carboxylic group from ground state cluster cations cannot explain experimentally observed yields of fragment ions at low collision energies. Therefore, we suggest that part of the M_n^+ that forms by cluster ion assembly in He droplets does not have the character of ground state valine cluster ions but may be already dissociated and matrix-stabilized complexes.

ASSOCIATED CONTENT

Supporting Information

The Supporting Information is available free of charge at https://pubs.acs.org/doi/10.1021/acs.jpca.0c07208.

Comparison between B3LYP+D2 and M06-2X functionals as well as Cartesian coordinates of all optimized structures (PDF)

https://dx.doi.org/10.1021/acs.jpca.0c07208
J. Phys. Chem. A 2020, 124, 8439–8445

AUTHOR INFORMATION

Corresponding Authors

Jaroslav Kočišek − *J. Heyrovský Institute of Physical Chemistry v.v.i., The Czech Academy of Sciences, Prague 18223, Czech Republic;* orcid.org/0000-0002-6071-2144; Email: jaroslav.kocisek@jh-inst.cas.cz

Paul Scheier − *Institut für Ionenphysik und Angewandte Physik, Universität Innsbruck, Innsbruck A-6020, Austria;* orcid.org/0000-0002-7480-6205; Email: paul.scheier@uibk.ac.at

Authors

Lukas Tiefenthaler − *Institut für Ionenphysik und Angewandte Physik, Universität Innsbruck, Innsbruck A-6020, Austria*

Milan Ončák − *Institut für Ionenphysik und Angewandte Physik, Universität Innsbruck, Innsbruck A-6020, Austria;* orcid.org/0000-0002-4801-3068

Siegfried Kollotzek − *Institut für Ionenphysik und Angewandte Physik, Universität Innsbruck, Innsbruck A-6020, Austria*

Complete contact information is available at: https://pubs.acs.org/10.1021/acs.jpca.0c07208

Notes

The authors declare no competing financial interest.

ACKNOWLEDGMENTS

This work was supported by the Austrian Science Fund, project number P31149, and the European Regional Development Fund (EFRE K-Regio FAENOMENAL, project no. EFRE 2016-4). J.K. acknowledges the support from the Czech Ministry of Education Youth and Sports via OP RDE. grant no. CZ.02.2.69/0.0/16 027/0008355. The computational results presented have been achieved using the HPC infrastructure LEO of the University of Innsbruck.

REFERENCES

(1) Yamashita, M.; Fenn, J. B. Electrospray Ion Source. Another Variation on the Free-Jet Theme. *J. Phys. Chem.* **1984**, *88*, 4451−4459.

(2) Fenn, J. B.; Mann, M.; Meng, C. K.; Wong, S. F.; Whitehouse, C. M. Electrospray Ionization−Principles and Practice. *Mass Spectrom. Rev.* **1990**, *9*, 37−70.

(3) Rizzo, T. R.; Stearns, J. A.; Boyarkin, O. V. Spectroscopic Studies of Cold, Gas-Phase Biomolecular Ions. *Int. Rev. Phys. Chem.* **2009**, *28*, 481−515.

(4) Roithová, J.; Gray, A.; Andris, E.; Jašík, J.; Gerlich, D. Helium Tagging Infrared Photodissociation Spectroscopy of Reactive Ions. *Acc. Chem. Res.* **2016**, *49*, 223−230.

(5) Tiefenthaler, L.; Ameixa, J.; Martini, P.; Albertini, S.; Ballauf, L.; Zankl, M.; Goulart, M.; Laimer, F.; von Haeften, K.; Zappa, F.; Scheier, P. An Intense Source for Cold Cluster Ions of a Specific Composition. *Rev. Sci. Instrum.* **2020**, *91*, No. 033315.

(6) Davies, J. A.; Besley, N. A.; Yang, S.; Ellis, A. M. Probing Elusive Cations: Infrared Spectroscopy of Protonated Acetic Acid. *J. Phys. Chem. Lett.* **2019**, *10*, 2108−2112.

(7) Franke, P. R.; Brice, J. T.; Moradi, C. P.; Schaefer, H. F., III; Douberly, G. E. Ethyl + O2 in Helium Nanodroplets: Infrared Spectroscopy of the Ethylperoxy Radical. *J. Phys. Chem. A* **2019**, *123*, 3558−3568.

(8) Abdoul-Carime, H.; Sanche, L. Alteration of Protein Constituents Induced by Low Energy <40 eV Electrons III. The Aliphatic Amino Acids. *J. Phys. Chem. B* **2004**, *108*, 457−464.

(9) Arumainayagam, C. R.; Lee, H.-L.; Nelson, R. B.; Haines, D. R.; Gunawardane, R. P. Low-Energy Electron-Induced Reactions in Condensed Matter. *Surf. Sci. Rep.* **2010**, *65*, 1−44.

(10) Junk, G.; Svec, H. The Mass Spectra of the -Amino Acids. *J. Am. Chem. Soc.* **1963**, *85*, 839−845.

(11) Papp, P.; Shchukin, P.; Kočíšek, J.; Matejčík, Š. Electron Ionization and Dissociation of Aliphatic Amino Acids. *J. Chem. Phys.* **2012**, *137*, 105101.

(12) Poully, J.-C.; Vizcaino, V.; Schwob, L.; Delaunay, R.; Kocisek, J.; Eden, S.; Chesnel, J.-Y.; Méry, A.; Rangama, J.; Adoui, L.; et al. Formation and Fragmentation of Protonated Molecules after Ionization of Amino Acid and Lactic Acid Clusters by Collision with Ions in the Gas Phase. *ChemPhysChem* **2015**, *16*, 2389−2396.

(13) Denifl, S.; Mähr, I.; Ferreira da Silva, F.; Zappa, F.; Märk, T. D.; Scheier, P. Electron Impact Ionization Studies with the Amino Acid Valine in the Gas Phase and (Hydrated) in Helium Droplets. *Eur. Phys. J. D* **2009**, *51*, 73−79.

(14) Lalanne, M. R.; Achazi, G.; Reichwald, S.; Lindinger, A. Association of Amino Acids Embedded in Helium Droplets Detected by Mass Spectrometry. *Eur. Phys. J. D* **2015**, *69*, 280.

(15) Weinberger, N.; Ralser, S.; Renzler, M.; Harnisch, M.; Kaiser, A.; Denifl, S.; Böhme, D. K.; Scheier, P. Ion Formation Upon Electron Collisions with Valine Embedded in Helium Nanodroplets. *Eur. Phys. J. D* **2016**, *70*, 91.

(16) Jochims, H.-W.; Schwell, M.; Chotin, J.-L.; Clemino, M.; Dulieu, F.; Baumgärtel, H.; Leach, S. Photoion Mass Spectrometry of Five Amino Acids in the 6−22 eV Photon Energy Range. *Chem. Phys.* **2004**, *298*, 279−297.

(17) Toennies, J. P.; Vilesov, A. F. Superfluid Helium Droplets: A Uniquely Cold Nanomatrix for Molecules and Molecular Complexes. *Angew. Chem., Int. Ed.* **2004**, *43*, 2622−2648.

(18) Gomez, L. F.; Loginov, E.; Sliter, R.; Vilesov, A. F. Sizes of Large He Droplets. *J. Chem. Phys.* **2011**, *135*, 154201.

(19) Kramida, A.; Ralchenko, Yu.,; Reader, J.; NIST ASD Team, *NIST Atomic Spectra Database (ver. 5.7.1)*; [Online]. Available: https://physics.nist.gov/asd [2019, November 5]. National Institute of Standards and Technology: Gaithersburg, MD, 2019.

(20) Laimer, F.; Kranabetter, L.; Tiefenthaler, L.; Albertini, S.; Zappa, F.; Ellis, A. M.; Gatchell, M.; Scheier, P. Highly Charged Droplets of Superfluid Helium. *Phys. Rev. Lett.* **2019**, *123*, 165301.

(21) Mauracher, A.; Echt, O.; Ellis, A. M.; Yang, S.; Bohme, D. K.; Postler, J.; Kaiser, A.; Denifl, S.; Scheier, P. Cold Physics and Chemistry: Collisions, Ionization and Reactions Inside Helium Nanodroplets Close to Zero K. *Phys. Rep.* **2018**, *751*, 1−90.

(22) Tiefenthaler, L.; Kočišek, J.; Scheier, P. Cluster Ion Polymerization of Serine and Tryptophan, the Water Loss Channel. *Eur. Phys. J. D* **2020**, *74*, 85.

(23) Klassen, J. S.; Kebarle, P. Collision-Induced Dissociation Threshold Energies of Protonated Glycine, Glycinamide, and Some Related Small Peptides and Peptide Amino Amides. *J. Am. Chem. Soc.* **1997**, *119*, 6552−6563.

(24) Tolmachev, A. V.; Vilkov, A. N.; Bogdanov, B.; PÄsa-Tolić, L.; Masselon, C. D.; Smith, R. D. Collisional Activation of Ions in RF Ion Traps and Ion Guides: The Effective Ion Temperature Treatment. *J. Am. Soc. Mass Spectrom.* **2004**, *15*, 1616−1628.

(25) Magnera, T. F.; David, D. E.; Stulik, D.; Orth, R. G.; Jonkman, H. T.; Michl, J. Production of Hydrated Metal Ions by Fast Ion or Atom Beam Sputtering. CollisionInduced Dissociation and Successive Hydration Energies of Gaseous Copper+ with 1-4 Water Molecules. *J. Am. Chem. Soc.* **1989**, *111*, 5036−5043.

(26) Zhao, Y.; Truhlar, D. G. The M06 Suite of Density Functionals for Main Group Thermochemistry, Thermochemical Kinetics, Noncovalent Interactions, Excited States, and Transition Elements: Two New Functionals and Systematic Testing of Four M06-class Functionals and 12 Other Functionals. *Theor. Chem. Acc.* **2008**, *119*, 215−241.

(27) Grimme, S. Semiempirical GGA-Type Density Functional Constructed with a LongRange Dispersion Correction. *J. Comput. Chem.* **2006**, *27*, 1787−1799.

(28) Frisch, M. J.; Trucks, G. W.; Schlegel, H. B.; Scuseria, G. E.; Robb, M. A.; Cheeseman, J. R.; Scalmani, G.; Barone, V.; Petersson,

G. A.; Nakatsuji, H. et al. *Gaussian 16*; Revision A.03., Gaussian Inc.: Wallingford CT, 2016.
(29) Breneman, C. M.; Wiberg, K. B. Determining Atom-Centered Monopoles from Molecular Electrostatic Potentials. The Need for High Sampling Density in Formamide Conformational Analysis. *J. Comput. Chem.* **1990**, *11*, 361−373.
(30) Beranova, S.; Cai, J.; Wesdemiotis, C. Unimolecular Chemistry of Protonated Glycine and Its Neutralized Form in the Gas Phase. *J. Am. Chem. Soc.* **1995**, *117*, 9492−9501.
(31) O'Hair, R. A. J.; Broughton, P. S.; Styles, M. L.; Frink, B. T.; Hadad, C. M. The Fragmentation Pathways of Protonated Glycine: a Computational Study. *J. Am. Soc. Mass Spectrom.* **2000**, *11*, 687−696.

https://dx.doi.org/10.1021/acs.jpca.0c07208
J. Phys. Chem. A 2020, 124, 8439−8445